ACS APPLIED MATERIALS & INTERFACES

Research Article

www.acsami.org

Reduced Graphene Oxide-Silver Nanoparticle Composite as Visible Light Photocatalyst for Degradation of Colorless Endocrine Disruptors

Susanta Kumar Bhunia and Nikhil R. Jana*

Centre for Advanced Materials, Indian Association for the Cultivation of Science, Kolkata 700032, India

Supporting Information

ABSTRACT: Sunlight-induced degradation of organic pollutants is an ideal approach for environmental pollution control and wastewater treatment. Although a variety of photocatalysts have been designed toward this goal, efficient degradation of colorless organic pollutants by visible light is a challenging issue. Here, we show that a reduced graphene oxide (rGO)-based composite with silver nanoparticle (rGO–Ag) can act as an efficient visible-light photocatalyst for the degradation of colorless organic pollutants. We have developed a simple, large-scale synthesis method for rGO–Ag and used it for the degradation of three well-known endocrine disruptors (phenol, bisphenol A, and atrazine) under UV and visible light. It is found that photocatalytic efficiency by rGO–Ag under visible light is significantly higher compared to that of rGO or silver nanoparticles. It is proposed that Ag nanoparticles offer visible-light-induced excitation of silver plasmons, and conductive rGO offers efficient charge separation and thus induces oxidative degradation of the organic pollutant. This approach can be extended for sunlight-induced degradation of different organic pollutants.

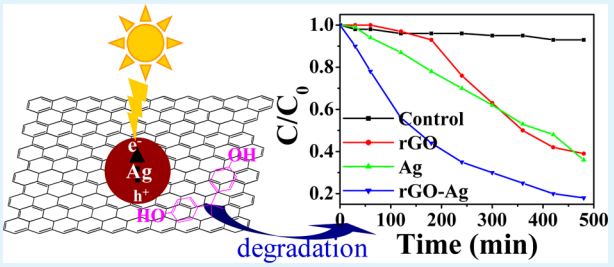

KEYWORDS: *reduced graphene oxide, nanoparticle, surface plasmon, photocatalysis, pollutant, endocrine disruptor*

INTRODUCTION

A wide variety of organic pollutants are responsible for environmental and water pollution.[1] These pollutants cause various environmental and health-related issues worldwide. In particular, a class of organic pollutants known as endocrine disruptors can interfere with hormone systems, resulting in reproductive problem, cancer, hypospadias, miscarriages, endomertriosis, and infertility.[2] Thus, efficient removal/degradation of organic pollutants is an important issue in environmental pollution monitoring and water purification.[3] Several methods exist for their separation, and among them, adsorption-based separation is most widely used due to its simplicity and general applicability.[3−5] However, separation efficiency varies depending on the chemical and physical nature of sorbents and pollutants.[3−5]

Sunlight-induced degradation of organic pollutants is one of the most attractive approaches for combating environmental pollution and wastewater treatment.[6] A variety of photocatalysts have been developed toward this goal. Among them, TiO_2 is most frequently used because of its chemical stability, favorable optoelectronic properties, low toxicity, and low cost.[7] However, TiO_2 is photoactive in the UV region due to its higher band gap (3.2 eV), and thus, utilization of solar irradiation is not efficient.[7] A variety of new generation visible-light photocatalysts are under development, and prominent examples include nitrogen -doped TiO_2,[8] plasmonic nanoparticle−TiO_2 composite,[9−11] plasmonic nanoparticle−quantum dot composite,[12] and other nanocomposites.[13−19] In addition, attempts have also been made to design catalysts with efficient charge separation and storage from the photoexcited nanoparticle, and prominent examples include Ag−TiO_2,[9] graphene−TiO_2,[20] graphene−quantum dot.[21]

Graphene-based composite with plasmonic and semiconductor nanoparticles offers unique advantage as a photocatalyst for organic pollutants.[22] Nanoparticles and graphene can acts as antennae for visible light. In addition, the highly conducting graphene surface offers high mobility of photogenerated charge carrier that in turn slows the recombination of photogenerated electron−hole pairs.[22] A hydrophobic graphene surface also offers the adsorption sites of organic molecules.[23] All these factors result in the enhancement of photocatalytic activity.[22] Although there are few reports on graphene−nanoparticle composite as visible-light photocatalyst they are mostly demonstrated for dye degradation, and reports on the degradation of colorless organics are rare or inefficient.[13−19] However, many organic pollutants are colorless and do not absorb visible light, and thus, visible-light-induced degradation is a challenging issue.[1] In this work, we show that reduced graphene oxide (rGO)-based composite with silver nanoparticle (rGO–Ag) can act as efficient visible-light photo-

Received: August 22, 2014
Accepted: October 8, 2014
Published: October 8, 2014

   dx.doi.org/10.1021/am505677x | ACS Appl. Mater. Interfaces 2014, 6, 20085−20092

Scheme 1. Synthetic Route for the Fabrication of Reduced Graphene Oxide−Silver Nanoparticle (rGO−Ag) Composite and Photocatalytic Degradation Strategy for Endocrine Disruptors

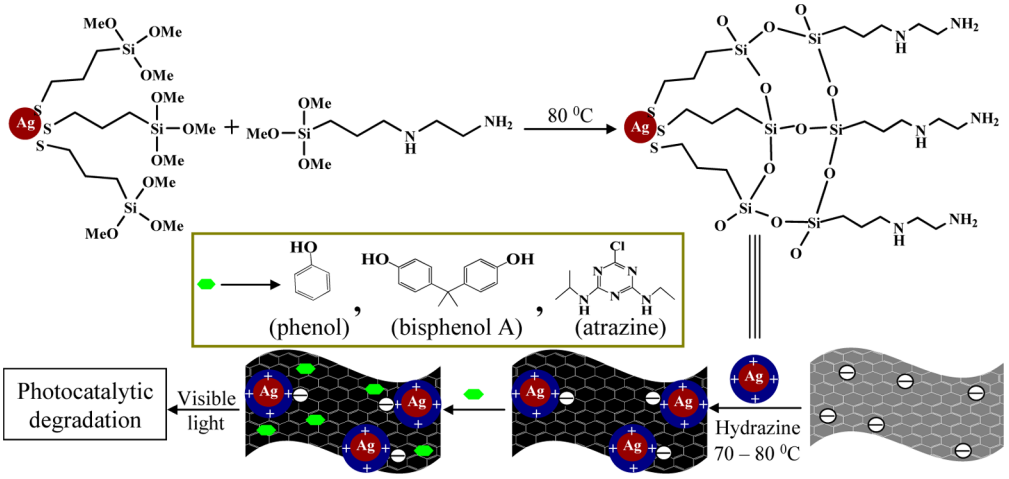

catalyst for degradation of colorless organic pollutants. We have developed a simple, low-cost, gram-scale synthesis method for rGO−Ag and used the composite for degradation of three well-known endocrine disruptors that are colorless. It is found that photocatalytic efficiency by rGO−Ag under visible light is significantly higher as compared to rGO or silver nanoparticle and depends on the optimum loading of Ag on rGO−Ag.

There are three distinct novelties of the presented approach. First, rGO−Ag has been synthesized by simple electrostatic interaction between negatively charged graphene oxide and silica-coated positively charged Ag nanoparticles followed by the hydrazine-based reduction of graphene oxide. The synthetic approach can finely control the loading of Ag nanoparticles, has been used for gram-scale synthesis of rGO−Ag, and can be easily adapted for even larger-scale synthesis. Second, the plasmonic property of Ag has been used for the efficient capturing of visible light and the photolysis of organic molecules that do not absorb any visible light. This approach can be used for the degradation of colorless organic pollutants Third, it is found that photocatalytic efficiency depends on loading of Ag, and loading that is either too high or too low reduces the catalytic activity. This work shows that controlled loading of plasmonic nanoparticles on a graphene surface is an important aspect for the effective utilization of visible light.

EXPERIMENTAL SECTION

Materials. Graphite powder (<20 μm), silver acetate (CH_3COOAg), tetrabutylammonium borohydride (TBAB), (3-mercaptopropyl)-trimethoxysilane (MPS), [3-(2-aminoethylamino)-propyl]trimethoxysilane (AEAPS), octylamine, oleic acid, hydrazine hydrate (98%), bisphenol A, and atrazine were purchased from Sigma-Aldrich. Phenol and potassium permanganate were purchased from Merck.

Preparation of Graphene Oxide (GO). Graphene oxide was prepared by modified Hummer's method according to previous reports.[24] Briefly, 200 mg of graphite powder, 100 mg of sodium nitrate, and ∼5 mL of concentrated H_2SO_4 were mixed in a beaker and cooled to 0 °C. Then, 600 mg of $KMnO_4$ was added in a stepwise manner to the cooled solution under vigorous stirring condition so that the temperature would not exceed 20 °C. After the complete addition of $KMnO_4$, the temperature of the solution was raised to 35 °C and kept there for half an hour. Next, 10 mL of water was added to the brownish gray paste, and the temperature of the solution rose to 98 °C. This temperature was maintained for 15 min, and then the whole solution was mixed with 30 mL of water to dilute it further. Afterward, 500 μL of 3% H_2O_2 was added to reduce the residual permanganate. The suspension turned light yellow in color. This was washed with warm water thoroughly for 7−8 times. The solid was air-dried and dissolved in distilled water by sonication for 30 min. Then, it was centrifuged at 3000 rpm for 30 min to remove large particles. The supernatant obtained is used as GO solution.

Synthesis of Water-Soluble Silica Coated Ag Nanoparticle. Water-soluble Ag nanoparticles were prepared according to an earlier report.[25] Briefly, 4.25 mg of CH_3COOAg was taken in 2.5 mL of toluene and dissolved in 50 μL of octylamine. Next, 25 μL of oleic acid and 50 μL of toluene solution of MPS (0.1 M) were added under stirring conditions. Then, 250 μL of toluene solution of TBAB (0.1 M) was added as a reducing agent, and the color of the solution changed to brown due to the formation of Ag nanoparticles. Next, 0.5 mL of toluene solution of AEAPS (0.1 M) was added to this solution, and the whole solution was heated at ∼65−70 °C for about half an hour until complete precipitation occurred. Then, the solution was centrifuged, and the precipitate was washed with toluene several times and solubilized in 2 mL of distilled water.

Preparation of Reduced Graphene Oxide−Silver Nanoparticle (rGO−Ag) Composite. rGO−Ag is synthesized according to our reported method with a finer adjustment of silver loading.[26] Typically, three separate batches of 50 mL of GO aqueous solution were prepared with a concentration of GO of ∼1 mg/mL and kept under stirring condition. Next, 25, 12, and 6 mL of aqueous silica-coated Ag nanoparticle solution (concentration ∼1 mg/mL) were added dropwise to three different vials. The solutions were stirred continuously for 15 min, and then 0.5 mL hydrazine hydrate solution was added to each batch and heated at ∼70−80 °C for 2 h. As time progressed, the brown colored solution turned black, and a precipitate formed. The black precipitate was washed with distilled water several times and dried. The dried composites were designated as rGO−Ag with rGO/Ag weight ratios of 1:0.5, 1:0.25, and 1:0.12, respectively. This approach was also used for larger scale preparation of rGO−Ag composites. For example, 60 mL of aqueous silica-coated Ag nanoparticle solution (concentration ∼2 mg/mL) was added dropwise to 250 mL of GO solution (concentration ∼2 mg/mL) under stirring condition. Stirring was continued for 15 min, and then 5 mL of hydrazine hydrate solution was added and heated at ∼70−80 °C for 2 h. Finally, black precipitate of rGO−Ag (with rGO/Ag = 1:0.25) was washed with distilled water several times and dried with a yield of ∼0.6 g.

Photocatalytic Experiment. Phenol, bisphenol A, and atrazine were selected as model endocrine disruptors to evaluate the catalytic performance of the prepared composites. In a typical process, 22 mg of rGO−Ag composite was dispersed in the 50 mL of pollutant solution with a concentration of 100 mg/L. The suspension was stirred in the dark for 2 h to establish adsorption−desorption equilibrium and then

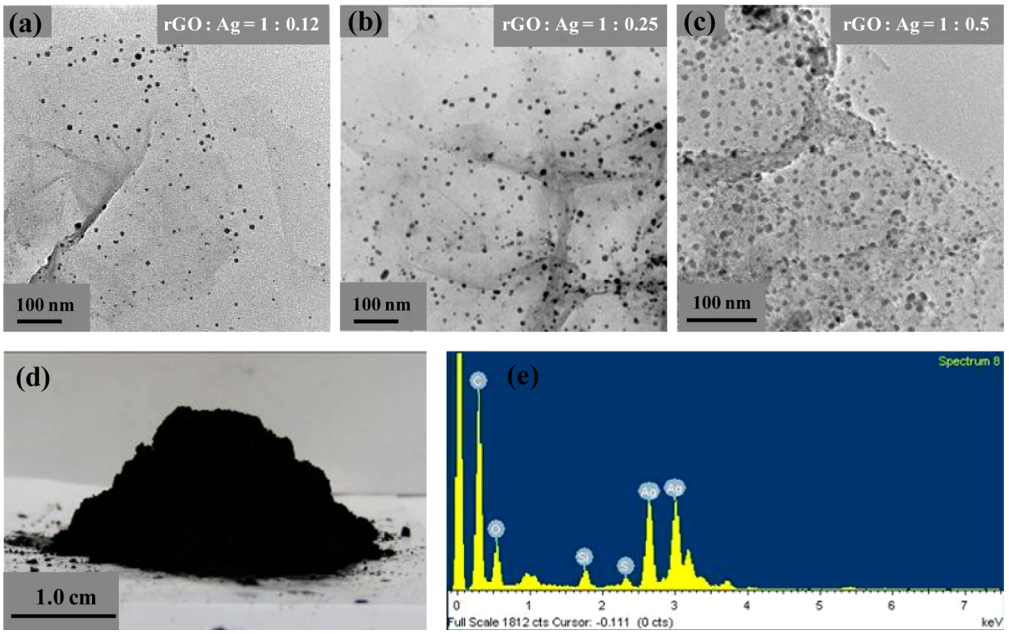

Figure 1. (a–c) TEM images of rGO–Ag composites with varied weight percent of Ag. (d) Digital image of large-scale solid rGO–Ag composite. (e) EDX of rGO–Ag composite indicating the presence of silver, silicon, and other elements.

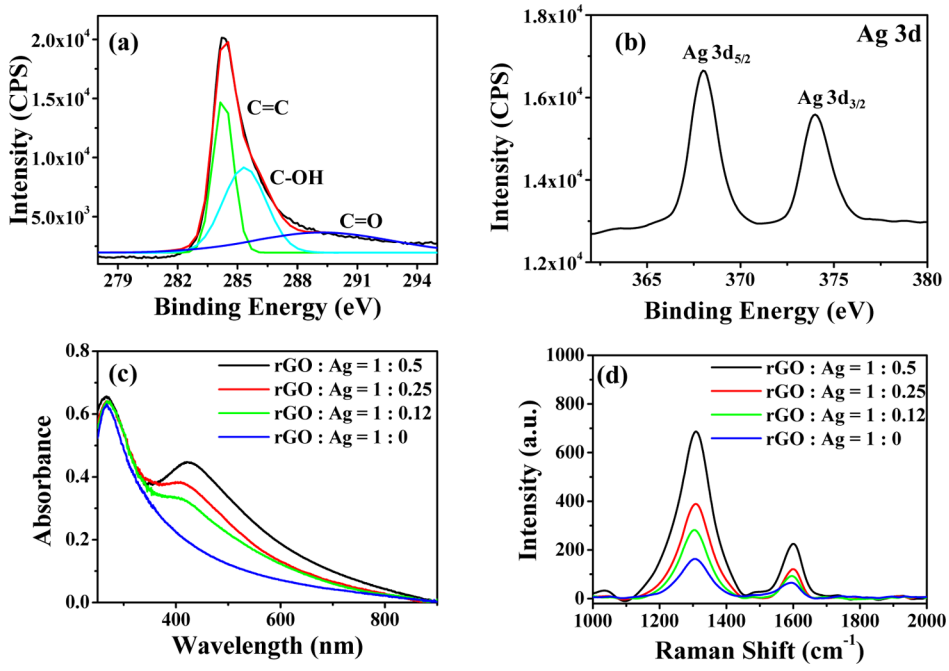

Figure 2. (a) Deconvoluted C 1s XPS spectrum displaying three peaks at ~284, ~ 286, and ~289 eV attributed to carbon with C=C, C–OH, and C=O groups, respectively. (b) Ag 3d XPS with intense doublet peaks at ~368 and ~374 eV corresponding to Ag $3d_{5/2}$ and Ag $3d_{3/2}$, respectively, of metallic Ag (0). (c) UV–vis absorption spectra of rGO–Ag with varying Ag weight percent, showing that silver plasmon peak at ~420 nm becomes more prominent with increasing Ag nanoparticle amount. (d) Raman spectra of various composites where the prominent G band at ~1600 cm^{-1} corresponds to sp^2 hybridized carbon atoms, and the D band at ~1310 cm^{-1} corresponds to a defect or disorder of the sp^2 hybridized carbon atoms.

irradiated with visible/UV light. A 250 W Hg vapor lamp was used for visible light irradiation source (light intensity ~5 mW/cm^2), whereas two 11 W UV lamp was used for UV light source (light intensity ~0.5 mW/cm^2). At different time intervals, a certain volume of aliquot was withdrawn, and rGO–Ag was separated by centrifuge. The aqueous solution was shaken well with an equal volume of $CHCl_3$, and the $CHCl_3$ extract was used to measure the concentration of residual pollutant by UV–visible spectroscopy.

Detection of Hydroxyl Radicals (OH•). Typically, 22 mg of the rGO–Ag was suspended in a 50 mL aqueous terephthalic acid solution (5×10^{-4} M), and the pH was adjusted to basic using NaOH solution. The solution was stirred for 2 h to reach homogeneity at room temperature. After that, the solution was irradiated with a 250 W Hg vapor lamp. A part of solution was collected at different time intervals and centrifuged to separate the photocatalyst, and finally, fluorescence of the solution was measured by exciting at 315 nm.

Instrumentation. Transmission electron microscopic (TEM) samples were prepared by putting a drop of composite suspension on a carbon-coated copper grid and observed with FEI Tecnai G2 F20 microscope. The field emission scanning electron microscopy

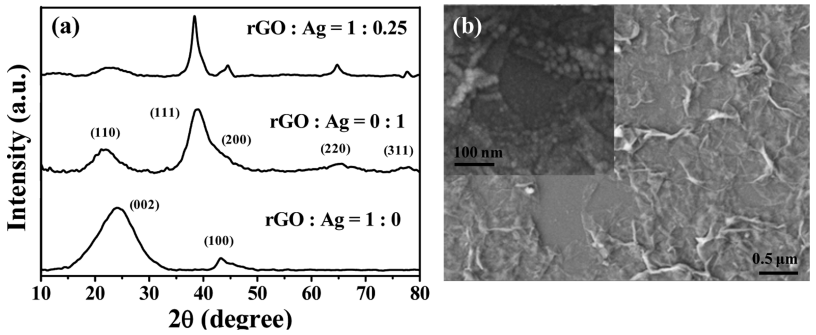

Figure 3. (a) XRD patterns of rGO, Ag, and rGO−Ag composite showing characteristic reflections for rGO and silver planes. (b) FESEM image of rGO−Ag showing the composite structure.

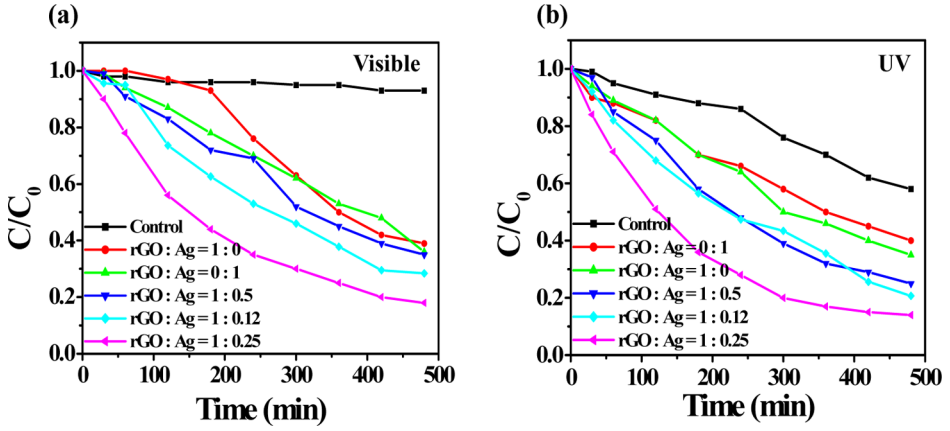

Figure 4. Photocatalytic degradation of phenol under (a) visible and (b) UV light irradiation using rGO−Ag composite with varying amounts of Ag showing that a rGO/Ag ratio of 1:0.25 displays higher photocatalytic activity than the other composites, only rGO nanoparticles, or only Ag nanoparticles. The control study indicates photolysis without any catalyst.

(FESEM) was performed with a Supra 40, Carl Zeiss, Pvt., Ltd. instrument. X-ray photoelectron spectroscopy (XPS) was measured using an Omicron (Serial No. 0571) X-ray photoelectron spectrometer by drop casting the dispersed solution on an indium tin oxide (ITO)-coated glass slide. Raman spectra were collected using an Agiltron R3000 Raman spectrometer with 785 nm excitation laser. Fourier transform infrared (FTIR) spectroscopy was performed with a PerkinElmer Spectrum 100 FTIR spectrometer using pellets made with solid KBr. UV−vis absorption spectra of dilute samples were collected using Shimadzu UV-2550 UV−vis spectrophotometer. Emission spectra were measured using a Synergy Mx Multi-Mode Microplate Reader. X-ray diffraction (XRD) patterns were obtained using a Bruker D8 ADVANCE powder diffractometer. Thermogravimetric analysis (TGA) was measured using a TA SDT Q600 instrument. Light intensity was measured using UV light meter (model UV340A) and visible light meter (model HTC LX101).

RESULTS

Synthesis and Characterization of Reduced Graphene Oxide-Silver Nanoparticle (rGO−Ag) Composite. The synthesis approach has been shown in Scheme 1. Colloidal graphene oxide (GO) is negatively charged due to the presence of carboxylate groups, and silica-coated Ag nanoparticles are positively charged due to the presence of amine groups.[26] When a colloidal solution of GO is added to a colloidal solution of Ag nanoparticles, electrostatic attraction leads to the attachment of cationic Ag nanoparticles on the anionic GO surface, and resultant composites precipitate from solution. Next, hydrazine is added followed by mild heating. Under this condition, most of the oxygen functional groups of GO are eliminated with the formation of chemically reduced graphene.[24] However, interaction between two the components still occurs due to the remaining carboxylate groups, and some epoxide groups of GO may covalently react with the primary amine groups of the silica shell.[27] The resultant rGO−Ag composite was isolated as a solid via simple centrifugation and washed with distilled water. The weight ratio of Ag nanoparticle to GO was varied to 1:0.5, 1:0.25, and 1:0.12, and different rGO−Ag composites were fabricated.

Composite nature of rGO−Ag has been confirmed from the TEM study (Figure 1). The number of Ag nanoparticles attached per rGO increases with the increasing weight ratio of Ag. The average size of a Ag nanoparticle is ∼5 nm (Supporting Information, Figure S1) and remains same in the composite. Energy-dispersive X-ray spectroscopy (EDX) of G−Ag reveals the presence of carbon, silver, silicon, sulfur, and oxygen (Figure 1e). X-ray photoelectron spectra (XPS) of the G−Ag composite determine the chemical environment of carbon and Ag (Figure 2). The C 1s XPS spectrum can be deconvoluted into three components with peaks at ∼284 eV for C═C groups, ∼286 eV for C−OH groups, and ∼289 eV for C═O groups[28] (Figure 2a). The intense doublet peaks at ∼368 and ∼374 eV correspond to Ag $3d_{5/2}$ and Ag $3d_{3/2}$, respectively, which is ascribed to metallic Ag (0)[29] (Figure 2b). Besides carbon and silver, the other elements such as nitrogen, oxygen, and silicon are present in the rGO−Ag composite, which is evident from raw XPS data (Supporting Information, Figure S2).

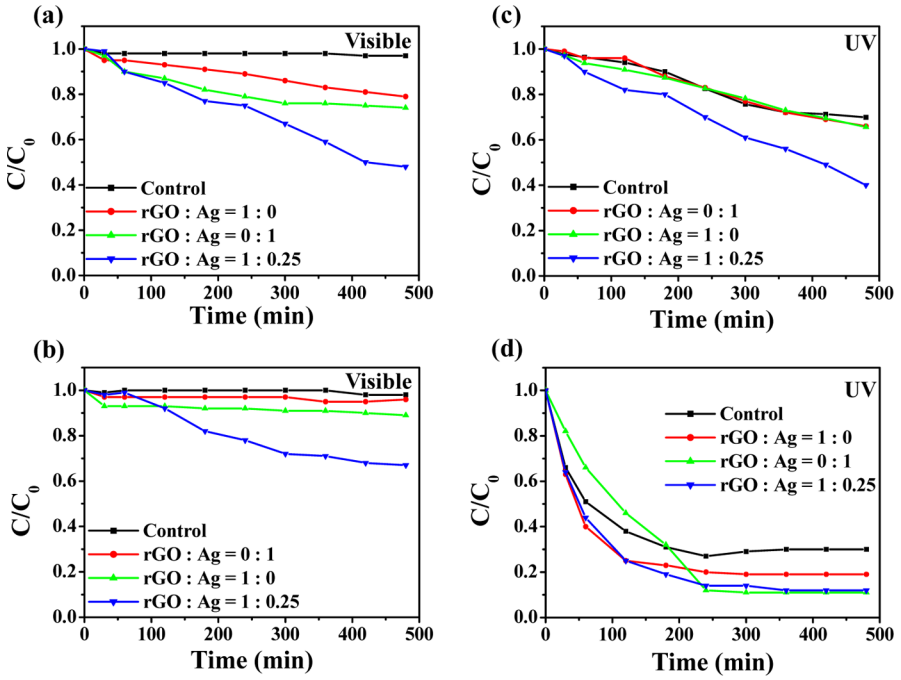

Figure 5. rGO−Ag composite with rGO/Ag of 1:0.25 as photocatalyst for degradation of (a and c) bisphenol A and (b and d) atrazine under (a and b) visible and (c and d) UV light.

The optical properties of rGO−Ag also indicate the property of both components. In Figure 2c, the prominent absorbance peak at ∼265 nm is due to $\pi-\pi^*$ transition of rGO component. The plasmonic peak of silver at ∼420 nm gradually becomes intense with increasing silver weight percent. Raman spectra of rGO−Ag composites shows a prominent G band at ∼1600 cm^{-1} corresponding to sp^2 hybridized carbon atoms and a D band at ∼1310 cm^{-1} corresponding to defective sp^2 hybridized carbon atoms in rGO[28] (Figure 2d). The large intensity ratio of the D band to G band (I_D/I_G, ∼ 3) for various rGO−Ag composites and higher value as compared to reduced graphene oxide (I_D/I_G ∼ 2.54) reflects the increased defects in rGO surface due to Ag nanoparticles.[28,29] XRD patterns of rGO−Ag show characteristic reflections due to rGO and silver (Figure 3a and Supporting Information, Figure S3).[28,29] The morphology of the composite has also been observed by FESEM (Figure 3b), which shows the attached Ag nanoparticles on the rGO sheet. The amount of Ag loading has been estimated by thermogravimetric study. Typically, ∼ 25 wt % of silver is present in rGO−Ag composite with 1:0.25 weight ratio of rGO to Ag nanoparticle (Supporting Information, Figure S4). FTIR data also shows the composite nature of rGO−Ag (Supporting Information, Figure S5)

Photocatalytic Degradation of Colorless Endocrine Disruptors. Three well-known endrocrine disruptor compounds such as phenol, bisphenol A, and atrazine have been selected for photocatalytic degradation study.[2] These three pollutants were selected because they are commonly found in wastewater with well-known toxic effect, and they do not absorb visible light.[2] Typically, an aqueous solution of endrocrine disruptor compound is mixed with solid rGO−Ag and stirred in the dark for 2 h to reach the equilibrium adsorption state. Next, the mixture solution is irradiated with visible or UV light, and a portion of the solution is used for quantitative investigation. Figures 4 and 5 summarize the results of photocatalytic degradation under visible and UV light.

The photocatalytic degradation result of phenol is shown in Figure 4. The initial concentration of phenol decreases with irradiation time, and the rate of photodegradation strongly depends on the nature of the light and of the catalyst. In the absence of any catalyst, phenol does not degrade under visible light but slowly degrades under UV light. The presence of catalyst initiates the degradation of phenol under visible light and enhances the rate of degradation under UV light. Most importantly, the visible-light-induced degradation of phenol by rGO−Ag is most effective compared to degradation by Ag nanoparticle or rGO. In addition, it is also observed that the rGO−Ag-based photocatalytic degradation rate is sensitive to Ag loading and is highest for rGO−Ag with a weight ratio of 1:0.25, but it is low for other compositions. A similar trend is observed for UV-light-induced photocatalytic degradation of phenol, suggesting that rGO−Ag is also most effective under UV light. Photocatalytic degradation of bisphenol A and atrazine shows that they do not degrade under visible light but degrade slowly under UV light (Figure 5). However, the degradation under visible light is most enhanced by rGO−Ag compared to rGO and Ag nanoparticle.

One of the important aspects of the catalyst is that it should be reused with unaltered performance. The presented catalyst is easily separable for reuse after the reaction via decantation or low-speed centrifugation. The visible-light photocatalytic performance of the rGO−Ag composite has been investigated by recycling it after the phenol degradation and then reusing it as catalyst. Results show that even after rGO−Ag is recycled five consecutive times, its photocatalytic activity does not significantly decrease (Figure 6). A TEM study of reused rGO−Ag shows that composite structure and Ag particle size remain intact (Supporting Information, Figure S6). This fact indicates that rGO−Ag is stable enough for repeated use.

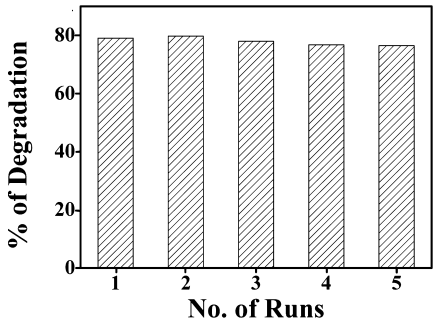

Figure 6. Photocatalytic degradation of phenol using recycled rGO–Ag composite five consecutive times, showing that catalytic activity does not decrease with repeated use.

DISCUSSION

Photocatalytic degradation of colorless endocrine disruptors is scientifically challenging, particularly because of two reasons: First, colorless organic pollutants do not absorb visible light, and thus, sunlight-induced photoexcitation followed by photodegradation is less effective. Second, colorless endocrine disruptors are generally present in low concentration in polluted water (typically millimolar to micromolar concentration), and at such low concentration, photodegradation requires very efficient catalyst.[1,2] Although efforts are made to develop photocatalysts that can degrade organic compounds under visible light,[13−19] in most cases, dyes have been used for degradation study, and it is proposed that dye can act as antennae for visible light.[30] These catalysts are expected to be less efficient for colorless endocrine disruptors.

Nanoparticle-based visible-light photocatalysis requires efficient capture of visible light, generation of electron–hole pairs, and effective use of electron, hole, or both before they recombine. However, the excitation recombination lifetime for a semiconductor nanoparticle is typically on the picosecond scale,[21] and for plasmonic nanoparticle it is on the femtosecond scale.[11] Thus, rapid excitation recombination leads to inefficient photocatalytic reactions. Here, we have selected graphene-based composite with Ag nanoparticle for two reasons. First, Ag nanoparticle can be used to capture visible light, and surface plasmon of silver nanoparticle can be tuned from visible to near-infrared by changing the particle size/shape. Second, composite with rGO can delay the recombination dynamics of plasmonic excitation, thereby offering efficient charge separation and photocatalytic reactions.

We have used a simple electrostatic-interaction-based approach to generate the rGO–Ag-based composite. The synthesis approach involves combination of two well-established methods: a one-step silica coating method to generate cationic Ag nanoparticle[25] and the preparation of chemically reduced graphene oxide from colloidal graphene oxide.[24] The electrostatic interaction between anionic graphene oxide and cationic Ag nanoparticle leads to the strong interaction between two components, and the presence of the Ag component inhibits the extensive rGO–rGO interaction. Thus, rGO surface is accessible for organic pollutants. In addition, a thin silica coating (~1–5 nm) offers a shorter distance between rGO and silver so that tunneling of photoexcited electron is possible.[25] The observed high performance of visible-light photocatalysis by rGO–Ag indicates that it actually serves the desired purpose. To further confirm that rGO–Ag is more efficient in producing intermediate hydroxyl radicals, we performed the visible-light photocatalytic reaction using terephthalic acid, which can trap the hydroxyl radicals[31,32] (Figure 7). Results show that rGO–Ag produces the highest concentration of hydroxyl radicals under similar conditions, compared to Ag nanoparticle or rGO. It is reported that rGO can capture visible light and acts as a photosensitizer under visible-light irradiation.[33] This property can explain the relatively high rate of photocatalysis by rGO. However, this rate of photocatalysis by rGO is slower than that for rGO–Ag.

A tentative mechanism of visible light photocatalytic degradation has been proposed on the basis of the observed results (Figure 8). The proposed mechanism considers Ag nanoparticles as antennae for visible light and rGO for efficient electron–hole separation. Visible light excite the Ag surface plasmon and this coherent oscillation of electrons produces high concentration of energetic electrons at Ag nanoparticle surface.[11] The conducting rGO surface adjacent to the Ag nanoparticle then quickly transports those electrons via its extended π-conjugation structure and leads to the efficient separation of electron–hole pairs.[34,35] This electron transfer phenomena is practically feasible because of the comparable work functions of Ag (4.2 eV) and rGO (4.48 eV).[36] Those electrons may react with dissolved oxygen to produce reactive oxygen species and holes on Ag can react with water molecules to produce hydroxyl radicals, and they are involved in the

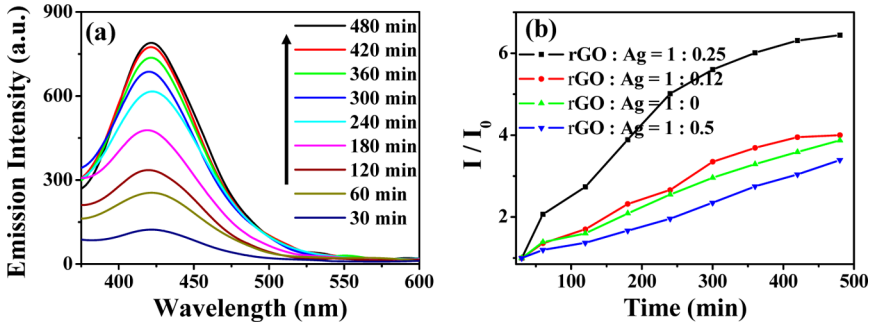

Figure 7. (a) Evidence of hydroxyl radical formation during photocatalysis. Photoluminescence spectra of terephthalic acid solution in the presence of rGO/Ag = 1:0.25 under increasing irradiation time of visible light. The gradual increase of the intensity at ~420 nm is due to the formation and trapping of hydroxyl radicals by terephthalic acid. (b) Extent of hydroxyl radical formation for different rGO–Ag photocatalyst as evidenced from the photoluminescence intensity of terephthalic acid. The highest intensity is observed for the catalyst with rGO/Ag = 1:0.25, suggesting that it produces the highest concentration of hydroxyl radicals.

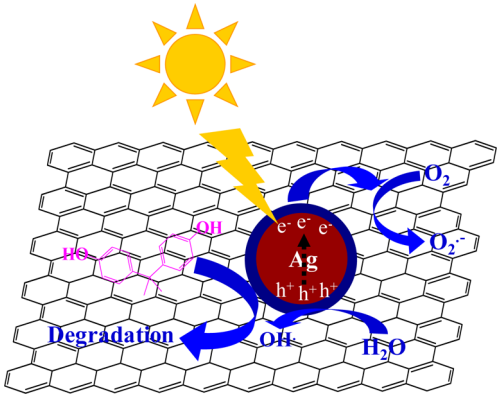

Figure 8. Proposed mechanism for photocatalytic degradation of endocrine disruptors by rGO−Ag catalyst under visible light.

degradation of organic pollutants.[31] In addition these reactive holes can directly oxidize pollutants.[37] The roles of these reactive oxygen species and hydroxyl radicals in photocatalytic degradation have been verified earlier by using different free radical scavengers (e.g., tert-butanol for $OH^{\bullet}$ scavenger, *p*-benzoquinone for $O_2^{\bullet-}$ scavenger, and disodium ethylenediaminetetraacetate as hole scavenger) that can block the photocatalysis.[33,37] Mechanistic studies show that organic molecules degrade into small molecules along with some intermediates.[38,39] The proposed mechanism is different from the earlier one in which organic molecules acts as antennae for visible light that transfer its excited electrons to plasmonic nanoparticles through rGO.[30] The proposed mechanism can explain the requirement of optimum loading of Ag nanoparticle. The loading of Ag nanoparticles controls the photoexcited electron−hole pairs, and the rest of the rGO surface is used for attachment of organic pollutants, and thus, optimum Ag loading can balance both requirements. At low Ag loading, the photocatalytic degradation is slow because low Ag does not produce sufficient reactive oxygen species. At high Ag loading, degradation is slow because pollutants can not absorb on graphene surface because they are blocked by Ag.

CONCLUSIONS

In conclusion, we propose reduced graphene-oxide-based composite with silver nanoparticle as a visible-light photocatalyst for efficient degradation of colorless organic pollutants. The synthesis method for this composite is simple and can be extended for large-scale synthesis. In the composite form, Ag nanoparticles act as antennae for visible light, and reduced graphene oxide offers efficient charge separation and acts as an adsorption site for organic pollutants. All these characteristic features make the composite a promising photocatalyst for the degradation of organic pollutants under visible light. This concept can be extended for the preparation of other plasmonic nanocomposites for visible-light photocatalysis.

ASSOCIATED CONTENT

Supporting Information

Summary of reported graphene-based nanocomposite for photocatalysis and characterization details of rGO−Ag composite. This material is available free of charge via the Internet at http://pubs.acs.org.

AUTHOR INFORMATION

Corresponding Author

*E-mail: camnrj@iacs.res.in Telephone: +91-33-24734971. Fax: +91-33-24732805.

Notes

The authors declare no competing financial interest.

ACKNOWLEDGMENTS

This work is financially supported by DST, Government of India. S.K.B. acknowledges CSIR India for research fellowship. Authors are thankful for support from the XPS facility of DST Unit of Nanoscience, IACS.

REFERENCES

(1) Benotti, M. J.; Trenholm, R. A.; Vanderford, B. J.; Holady, J. C.; Stanford, B. D.; Snyder, S. A. Pharmaceuticals and Endocrine Disrupting Compounds in U.S. Drinking Water. *Environ. Sci. Technol.* **2009**, *43*, 597−603.

(2) Boas, M.; Feldt-Rasmussen, U.; Main, K. M. Thyroid Effects of Endocrine Disrupting Chemicals. *Mol. Cell. Endocrionol.* **2012**, *355*, 240−248.

(3) Zhang, Y.; Causserand, C.; Aimar, P.; Cravedi, J. P. Removal of Bisphenol A by a Nanofiltration Membrane in View of Drinking Water Production. *Water Res.* **2006**, *40*, 3793−3799.

(4) Basile, T.; Petrella, A.; Petrella, M.; Boghetich, G.; Petruzzelli, V.; Colasuonno, S.; Petruzzelli, D. Review of Endocrine-Disrupting-Compound Removal Technologies in Water and Wastewater Treatment Plants: An EU Perspective. *Ind. Eng. Chem. Res.* **2011**, *50*, 8389−8401.

(5) Sui, Q.; Huang, J.; Liu, Y. S.; Chang, X. F.; Ji, G. B.; Deng, S. B.; Xie, T.; Yu, G. Rapid Removal of Bisphenol A on Highly Ordered Mesoporous Carbon. *J. Environ. Sci.* **2011**, *23*, 177−182.

(6) Keane, D. A.; McGuigan, K. G.; Ibanez, P. F.; Polo-Lopez, M. I.; Byme, J. A.; Dunlop, P. S. M.; O'Shea, K.; Dionysiou, D. D.; Pillai, S. C. Solar Photocatalysis for Water Disinfection: Materials and Reactor Design. *Catal. Sci. Technol.* **2014**, *4*, 1211−1226.

(7) Linsebigler, A. L.; Lu, G. Q.; Yates, J. T. Photocatalysis on TiO_2 Surfaces—Principles, Mechanisms, and Selected Results. *Chem. Rev.* **1995**, *95*, 735−758.

(8) Asahi, R.; Morikawa, T.; Ohwaki, T.; Aoki, K.; Taga, Y. Visible-Light Photocatalysis in Nitrogen Doped Titanium Oxides. *Science* **2001**, *293*, 269−271.

(9) Takai, A.; Kamat, P. V. Capture, Store, and Discharge. Shuttling Photogenerated Electrons across TiO_2-Silver Interface. *ACS Nano* **2011**, *5*, 7369−7376.

(10) Kochuveedu, S. T.; Kim, D. P.; Kim, D. H. Surface-Plasmon-Induced Visible Light Photocatalytic Activity of TiO_2 Nanospheres Decorated by Au Nanoparticles with Controlled Configuration. *J. Phys. Chem. C* **2012**, *116*, 2500−2506.

(11) Kale, M. J.; Avanesian, T.; Christopher, P. Direct Photocatalysis by Plasmonic Nanostructures. *ACS Catal.* **2014**, *4*, 116−128.

(12) Costi, R.; Saunders, A. E.; Elmalem, E.; Salant, A.; Banin, U. Visible Light-Induced Charge Retention and Photocatalysis with Hybrid CdSe−Au Nanodumbbells. *Nano Lett.* **2008**, *8*, 637−641.

(13) Hu, C.; Lan, Y. Q.; Qu, J. H.; Hu, X. X.; Wang, A. M. Ag/AgBr/TiO_2 Visible Light Photocatalyst for Destruction of Azodyes and Bacteria. *J. Phys. Chem. B* **2006**, *110*, 4066−4072.

(14) Wang, P.; Huang, B. B.; Zhang, X. Y.; Qin, X. Y.; Jin, H.; Dai, Y.; Wang, Z. Y.; Wei, J. Y.; Zhan, J.; Wang, S. Y.; Wang, J. P.; Whangbo, M. H. Highly Efficient Visible-Light Plasmonic Photocatalyst Ag@AgBr. *Chem.—Eur. J.* **2009**, *15*, 1821−1824.

(15) Zhang, H.; Fan, X. F.; Quan, X.; Chen, S.; Yu, H. T. Graphene Sheets Grafted Ag@AgCl Hybrid with Enhanced Plasmonic Photocatalytic Activity under Visible Light. *Environ. Sci. Technol.* **2011**, *45*, 5731−5736.

(16) Liu, Y. P.; Fang, L.; Lu, H. D.; Li, Y. W.; Hu, C. Z.; Yu, H. G. One-Pot Pyridine-Assisted Synthesis of Visible-Light-Driven Photocatalyst Ag/Ag_3PO_4. *Appl. Catal., B* **2012**, *115*−*116*, 245−252.
(17) Liu, Y. P.; Fang, L.; Lu, H. D.; Liu, L. J.; Wang, H.; Hu, C. Z. Highly Efficient and Stable Ag/Ag_3PO_4 Plasmonic Photocatalyst in Visible Light. *Catal. Commun.* **2012**, *17*, 200−204.
(18) Zhang, H. C.; Huang, H.; Ming, H.; Li, H. T.; Zhang, L. L.; Liu, Y.; Kang, Z. H. Carbon Quantum Dots/Ag_3PO_4 Complex Photocatalysts with Enhanced Photocatalytic Activity and Stability under Visible Light. *J. Mater. Chem.* **2012**, *22*, 10501−10506.
(19) Wang, P. H.; Tang, Y. X.; Dong, Z. L.; Chen, Z.; Lim, T. T. Ag−AgBr/TiO_2/RGO Nanocomposite for Visible-Light Photocatalytic Degradation of Penicillin G. *J. Mater. Chem. A* **2013**, *1*, 4718−4727.
(20) Zhang, Y. H.; Tang, Z. R.; Fu, X. Z.; Xu, Y. J. TiO_2-Graphene Nanocomposites for Gas-Phase Photocatalytic Degradation of Volatile Aromatic Pollutant: Is TiO_2−Graphene Truly Different from Other TiO_2−Carbon Composite Materials? *ACS Nano* **2010**, *4*, 7303−7314.
(21) Kaniyankandy, S.; Rawalekar, S.; Ghosh, H. N. Ultrafast Charge Transfer Dynamics in Photoexcited CdTe Quantum Dot Decorated on Graphene. *J. Phys. Chem. C* **2012**, *116*, 16271−16275.
(22) Kamat, P. V. Graphene-Based Nanoarchitectures. Anchoring Semiconductor and Metal Nanoparticles on a Two-Dimensional Carbon Support. *J. Phys. Chem. Lett.* **2010**, *1*, 520−527.
(23) Zhao, G. X.; Jiang, L.; He, Y. D.; Li, J. X.; Dong, H. L.; Wang, X. K.; Hu, W. P. Sulfonated Graphene for Persistent Aromatic Pollutant Management. *Adv. Mater.* **2011**, *23*, 3959−3963.
(24) Bhunia, S. K.; Jana, N. R. Peptide-Functionalized Colloidal Graphene via Interdigited Bilayer Coating and Fluorescence Turn-on Detection of Enzyme. *ACS Appl. Mater. Interfaces* **2011**, *3*, 3335−3341.
(25) Jana, N. R.; Earhart, C.; Ying, J. Y. Synthesis of Water-Soluble and Functionalized Nanoparticles by Silica Coating. *Chem. Mater.* **2007**, *19*, 5074−5082.
(26) Salam, N.; Sinha, A.; Roy, A. S.; Mondal, P.; Jana, N. R.; Islam, S. M. Synthesis of Silver−Graphene Nanocomposite and Its Catalytic Application for the One-Pot Three-Component Coupling Reaction and One-Pot Synthesis of 1,4-Disubstituted 1,2,3-Triazoles in Water. *RSC Adv.* **2014**, *4*, 10001−10012.
(27) Loh, K. P.; Bao, Q. L.; Ang, P. K.; Yang, J. X. The Chemistry of Graphene. *J. Mater. Chem.* **2010**, *20*, 2277−2289.
(28) Bhunia, S. K.; Saha, A.; Maity, A. R.; Ray, S. C.; Jana, N. R. Carbon Nanoparticle-Based Fluorescent Bioimaging Probes. *Sci. Rep.* **2013**, *3*, No. 1473.
(29) Mondal, A.; Jana, N. R. Surfactant-Free, Stable Noble Metal−Graphene Nanocomposite as High Performance Electrocatalyst. *ACS Catal.* **2014**, *4*, 593−599.
(30) Zhang, J. T.; Xiong, Z. G.; Zhao, X. S. Graphene−Metal−Oxide Composites for the Degradation of Dyes under Visible Light Irradiation. *J. Mater. Chem.* **2011**, *21*, 3634−3640.
(31) Wang, J. X.; Ruan, H.; Li, W. J.; Li, D. Z.; Hu, Y.; Chen, J.; Shao, Y.; Zheng, Y. Highly Efficient Oxidation of Gaseous Benzene on Novel Ag_3VO_4/TiO_2 Nanocomposite Photocatalysts under Visible and Simulated Solar Light Irradiation. *J. Phys. Chem. C* **2012**, *116*, 13935−13943.
(32) Chen, Y.; Huang, W.; He, D.; Situ, Y.; Huang, H. Construction of Heterostructured g-$C_3N_4/Ag/TiO_2$ Microspheres with Enhanced Photocatalysis Performance under Visible-Light Irradiation. *ACS Appl. Mater. Interfaces* **2014**, *6*, 14405−14414.
(33) Zhang, Y. H.; Zhang, N.; Tang, Z. R.; Xu, Y. J. Graphene Transforms Wide Band Gap ZnS to a Visible Light Photocatalyst. The New Role of Graphene as a Macromolecular Photosensitizer. *ACS Nano* **2012**, *6*, 9777−9789.
(34) Lightcap, I. V.; Kosel, T. H.; Kamat, P. V. Anchoring Semiconductor and Metal Nanoparticles on a Two-Dimensional Catalyst Mat. Storing and Shuttling Electrons with Reduced Graphene Oxide. *Nano Lett.* **2010**, *10*, 577−583.
(35) Mou, Z.; Wu, Y.; Sun, J.; Yang, P.; Du, Y.; Lu, C. TiO_2 Nanoparticles-Functionalized N-Doped Graphene with Superior Interfacial Contact and Enhanced Charge Separation for Photocatalytic Hydrogen Generation. *ACS Appl. Mater. Interfaces* **2014**, *6*, 13798−13806.
(36) Li, J.; Liu, C. Y. Ag/Graphene Heterostructures: Synthesis, Characterization, and Optical Properties. *Eur. J. Inorg. Chem.* **2010**, *2010*, 1244−1248.
(37) Yang, X. F.; Cui, H. Y.; Li, Y.; Qin, J. L.; Zhang, R. X.; Tang, H. Fabrication of Ag_3PO_4−Graphene Composites with Highly Efficient and Stable Visible Light Photocatalytic Performance. *ACS Catal.* **2013**, *3*, 363−369.
(38) Luna, A. J.; Nascimento, C. A. O.; Foletto, E. L.; Moraes, J. E. F.; Chiavone, O. Photo-Fenton Degradation of Phenol, 2,4-Dichlorophenoxyacetic Acid and 2,4-Dichlorophenol Mixture in Saline Solution using a Falling-Film Solar Reactor. *Environ. Technol.* **2014**, *35*, 364−371.
(39) Guo, C. S.; Ge, M.; Liu, L.; Gao, G. D.; Feng, Y. C.; Wang, Y. Q. Directed Synthesis of Mesoporous TiO_2 Microspheres: Catalysts and Their Photocatalysis for Bisphenol A Degradation. *Environ. Sci. Technol.* **2010**, *44*, 419−425.